applied sciences

Article

Comparison of Abrasive Wear Resistance of Hardox Steel and Hadfield Cast Steel

Martyna Zemlik [1,*], Łukasz Konat [1], Kacper Leśny [1] and Krzysztof Jamroziak [2,*]

1 Department of Vehicle Engineering, Faculty of Mechanical Engineering, Wroclaw University of Science and Technology, Wybrzeze Wyspianskiego 27 Str., 50-370 Wrocław, Poland; lukasz.konat@pwr.edu.pl (Ł.K.); kacper.lesny@pwr.edu.pl (K.L.)

2 Department of Mechanics, Materials and Biomedical Engineering, Faculty of Mechanical Engineering, Wrocław University of Science and Technology, Wybrzeze Wyspianskiego 27 Str., 50-370 Wroclaw, Poland

* Correspondence: martyna.zemlik@pwr.edu.pl (M.Z.); krzysztof.jamroziak@pwr.edu.pl (K.J.)

Abstract: Among the materials used for components subjected to abrasive wear, chromium cast iron, hardfaced layers, martensitic steels and Hadfield steel should be singled out. Each of these types of materials exhibits a different morphology of structure and strength properties. Hadfield steel, characterized by an austenitic microstructure, shows the ability to strengthen the subsurface layers by cold work, while maintaining a ductile core. Hardox steels belong to the group of low-alloy martensitic boron steels. However, it should be noted that increasing hardness does not always translate into low wear values due to a change in the nature of wear. In view of the above, the authors decided to subject selected Hardox steels and Hadfield cast steels in the post-operational condition to abrasive wear tests in the presence of loose abrasive. The study showed that Hardox Extreme steel exhibits the highest resistance to abrasive wear (value of the coefficient k_b is equal to 1.39). In the case of Hadfield steel, the recorded values are slightly lower (k_b = 1.32 and 1.33), while the above ratios remain higher compared to Hardox 600 and Hardox 500 steels. The main wear mechanism of high-manganese steels is microploughing, plastic deformation and breakouts of larger fragments of material. In the case of Hardox 450 and Hardox 500 steels, the predominant wear mechanisms are microploughing and breaking out of material fragments. As the hardness of the steel increases, the proportion of wear by microcutting and scratching predominates.

Keywords: Hadfield cast steel; Hardox steel; martensitic boron steel; abrasive wear

Citation: Zemlik, M.; Konat, Ł.; Leśny, K.; Jamroziak, K. Comparison of Abrasive Wear Resistance of Hardox Steel and Hadfield Cast Steel. *Appl. Sci.* **2024**, *14*, 11141. https://doi.org/10.3390/app142311141

Academic Editor: Andrea Carpinteri

Received: 21 September 2024
Revised: 23 October 2024
Accepted: 26 November 2024
Published: 29 November 2024

1. Introduction

The group of materials used for components subjected to abrasive wear includes martensitic steels, Hadfield steel, hard-faced materials and chromium cast iron. The selection of a specific material for components subjected to abrasive wear should take into account the analysis of complex operating conditions, and the fulfilment of specific operating requirements is determined by a number of microstructural and mechanical properties, which are defined by: the method of manufacture in the smelter or foundry, the chemical composition, the type and parameters of heat treatment, the type and size of the microstructure, hardness, tensile strength, yield strength, impact strength, elongation, percent reduction of area, susceptibility to work hardening, the type of transferred loads and the type of acting abrasive [1–4].

Hadfield steel is named after its discoverer, Robert Hadfield, who produced high-manganese steel in 1882. Its commercial success was due to its different mechanical properties compared to carbon steels, so the above date is considered the birth of alloy steels. At that time, Hadfield steel became a common application for components that, in addition to working under frictional conditions, are also exposed to significant surface pressures. The favourable properties of Hadfield cast steels are the result of its austenitic microstructure, which is made possible by the addition of carbon and manganese in a ratio of 1:10. Parts made of Hadfield cast steels are subjected to saturation treatments—during heating to a temperature of about 1000 °C, dissolution of the cementite occurs, and then, as a result of rapid cooling, a single-phase structure is obtained. This prevents the precipitation of manganese cementite $(Fe, Mn)_3C$ coexisting with ferrite. As a result of the technological procedure carried out in this way, Hadfield cast steel is characterized by a high rate of work hardening, which is a consequence of plastic deformation (TWIP effect) or the decomposition of austenite into martensite (TRIP effect). Under the influence of dynamic loads causing plastic deformation, the subsurface layers of the component become mechanically strong (an increase in hardness level from about 210 to 500 HBW is observed), while the core retains high plastic properties, i.e., impact strength and ductility. Since the significant tendency to work hardening results in limited opportunities for subtractive machining, the material is often cast. The commercial designation of Hadfield cast steel, taking into account the basic manganese addition of 12%, is X120Mn12 (steel) or L120G12M (casting). This material is used, among others, for railway switches, excavator baskets, jaw crushers or tractor track parts [5,6]. Currently, numerous studies are focusing on modifying the chemical composition of high-manganese steels by adding carbide-forming elements that improve abrasive wear resistance and ensure the preservation of the austenitic structure by blocking the precipitation of manganese cementite [7,8]. Moreover, Al addition is also advised to increase yield strength [9,10]. According to [11,12], the addition of vanadium at 8.1% and niobium at 4.5% can result in up to a threefold improvement in wear resistance during Miller slurry abrasivity tests. In the case of high-manganese steels, a separate problem is their tendency to become coarse-grained due to the lack of α -> γ transformation. The above issue can be resolved by heat treatment [13]. In this case, the recrystallized structure was obtained by a two-stage heat treatment that included a prolonged isothermal annealing at 510 °C to separate numerous pearlite grains, which, in the next stage, provided nuclei for austenite nucleation during heating to 900 °C. In this way, improved mechanical properties were obtained in comparison with single-stage austenitized steels.

Hardox steel was first produced in 1970 by Sweden's SSAB-Oxelösund. Today, the Hardox family of steels includes 10 grades, of which 2 are designed for special applications, involving elevated operating temperatures (Hardox HiTemp) and corrosive environments (Hardox HiAce) [14]. Hardox 450 steel is recommended as a highly versatile structural steel, showing high impact strength even at reduced temperatures. It is designed for components of concrete mixers, snow cannons, containers, excavator and loader buckets, grapples, shears, garbage trucks, dump trucks, drums, asphalt rollers, combines, recycling tools, crushers and chutes. Hardox 500 and 550 steels are designed for applications where there is heavy wear with limited material design requirements, such as lining plates of crushers and feeders and hammers used in recycling. Hardox 550 offers improved durability, replacing manganese steels. Hardox 600 is suitable for heavier duty, can be cut and welded and retains satisfactory impact strength despite its high hardness. It is used, for example, in moulds for brick making, for cladding and screed plates in mineral transportation and processing, in concrete mixers and for blades and knives for recycling. Hardox Extreme steel is described as the world's hardest wear-resistant steel with a nominal hardness of 60 HRC (650–700 HBW). Tests conducted in [15] showed that Hardox Extreme steel exhibits an average strength R_m = 2411 MPa and KCV $\approx$ 12 J/cm^2. It is designed for applications with extremely high wear resistance requirements, such as cladding plates. On the other hand, due to its low impact strength, some caution should be exercised when selecting Hardox Extreme steel for structural components. The key to determining areas of application for this steel is the $R_{p0.2}/R_m$ value of 0.64–0.74, which is only appropriate for structures requiring a low safety factor. At the same time, it should be mentioned here that the high $R_{p0.2}/R_m$ ratio is most often indicated by designers of primary machinery of the lignite mining industry as the main factor—in addition to weldability—limiting the use of high-strength, low-alloy steels for the construction of machines [3,16–18]. In terms of weldability, a separate problem is the lowering of the mechanical properties of the above-mentioned steels, both in the weld material zone and the broad heat-affected zone, which is due to their highest mechanical indices [19–22] among available steels and the maximum strength of 1000 MPa of commercially sold welding alloys. According to numerous contemporary papers [23–28], this problem can only be eliminated by using high-quality welding consumables and by means of subsequent heat treatment.

According to available tribological studies of martensitic boron steels, the condition for maintaining advantageous indices of abrasive wear resistance is to obtain a fine lath microstructure [4,29,30]. Moreover, the abrasion wear resistance of Hardox 500 steel can be more favourable compared to carburized 20MnCr5 steel [31]. Hardox 500 steel also shows lower weight loss compared to S355JR, S355J2 and AISI304 steels during tribological tests in the presence of garnet and carborundum [32]. On the other hand, in the available scientific literature, no information can be found on the results of tests to compare the abrasive wear resistance of high-manganese steels and martensitic steels. Since the selection of material for individual components depends on the nature of the loads acting on them and the type of excavated material (its hardness and volume), an individual approach to material proposals requires verification, among other things, of the behavior of materials under particular, well-defined abrasive wear conditions. For that purpose, a T-07 device for testing wear resistance in the presence of loose abrasive (electrocorundum) was used. It allowed for the determination of the coefficient of relative abrasion wear resistance k_b, which shows correlation as a preliminary test method with the results of field tests of ploughshares [33] and it can be used as a method for the selection of material for dozers [34]. The establishment of the above research methodology was due to the utilitarian aspect—the analyzed group of materials is used for parts of buckets for excavators and components of agricultural machinery, which work under intensive wear conditions in the mining of deposits and excavation of soil abrasive mass.

2. Materials and Methods

For abrasive wear testing of Hardox steel, 10-mm-thick steel sheets provided by the authorized distributor, STAL-HURT company, were used. On the other hand, samples for testing abrasive wear of Hadfield steel in the post-operational condition were taken from the following assemblies of mine machinery and equipment structures:

- material of the jaw crusher (Sample 1)
- ball mill liner plate material (Sample 2).

The above components come from one of the melaphyre mines located in Lower Silesia (Poland). Melaphyre belongs to magmatic rocks formed during the Palaeozoic period. In terms of quality, it corresponds to tertiary basalts and is a raw material for the production of various types of aggregates. These aggregates are produced in fractions from 2 to 63 mm. Their applications are very wide and apply to wearing layers, binders and substructures in road construction, aggregates for concrete, as well as aggregates for railroad ballast. After mining, melaphyre is crumbled using crushers, with the fastest consumable elements being their jaws. It is then ground into various fractions in ball mills (the critical elements are the liner plates). Subsequently, the excavated material is deposited in stockpiles through a system of conveyor belts and transfers (the critical elements of the transfers are the liner plates as well).

Figures 1 and 2 show macroscopic photos of the tested components in their post-operational state. As can be seen from the photographic documentation, the wear on the working surfaces of samples 1 and 2 consists of abrasion of their surfaces and a change in geometry—in the case of the jaw crusher, a reduction in the height of the protrusions on the working surface, and in the case of the ball mill liner plate, a fairly uniform ploughing. In both cases, no cracks of a macroscopic nature were found on the surfaces of these samples. While the changes in the condition of the working surface of the jaw crusher indicate the loss of the assumed properties, the condition of the surface of sample 2 suggests the possibility of the continued operation of the liner plate.

Figure 1. Sample 1. Macroscopic image of the condition of the working surface of the jaw crusher for squashing rocks with a volume of 10–1000 mm. Operating time of about 350 h, throughput of about 80.00 tons.

Figure 2. Sample 2. Macroscopic image of the surface condition of the ball mill liner plate covering part of the contracture of the chute. Material volume of 100–1200 mm, throughput of about 200.000 tons.

The hardness was measured using a Zwick/Roel ZHU 187.5 universal hardness tester (Zwick Roell Gruppe, Ulm, Germany) using the Brinell method, in accordance with PN-EN ISO 6506-1:2014-12 [35]. A carbide ball with a diameter of 2.5 mm was used, with a load of 187.5 kgf (1838.7469 N) applied for 15 s.

Analyses of chemical composition were carried out using the spectral method via a Leco GDS500A glow discharge emission analyser (LECO Corporation, St. Joseph, MI, USA). During the analyses, the following parameters were used to allow ionization of the inert gas: U = 1250 V, I = 45 mA, 99.999% argon. The obtained results were the arithmetic average of at least five measurements.

The results of chemical analyses of samples 1 and 2 confirm that the post-operational samples represent high-manganese cast steels (Table 1). The chemical composition of sample 2 met the requirements of PN-88/H-83160 standard [36], showing an overestimated (by 0.3%) content of chromium, which stabilizes the microstructure by blocking the separation of manganese cementite and increases wear resistance due to the presence of carbides. In sample 1, the manganese content (at 18%) was significantly higher than in in the case of sample number 2, while the chromium content was 1.8%. The established chemical composition of this material allows it to be classified as steel grade GX120MnCr 17-2, captured in the ISO 13521:1999 [37] standard. The differences in the chemical composition between samples 1 and 2 also resulted in a different level of hardness (sample 1–299 HBW, sample 2–256 HBW). The chemical composition of Hardox steels allows them to be classified as low-carbon (Hardox 450) and medium-carbon steels (Hardox 500, 600, Extreme). Increasing the amount of carbon lowers the austenite stability temperature, with a similar effect also exerted by non-carbide-forming elements, i.e., manganese, nickel and copper. The delay in diffusion transformation (the shift of the curves on the CTP diagram to the right) is the result of the use of both non-carbide- and carbide-forming elements, with manganese, molybdenum, chromium, silicon and nickel having the strongest effect on hardenability, respectively. The addition of boron in each of the analyzed steels occured in the maximum permissible concentration—0.002%. Larger amounts can cause coagulation of Fe_2B compounds which favour nucleation of the ferritic phase. The content of nickel, also added to lower the temperature of the ductile-brittle transition, was highest for Hardox 600 steel (2.03%). Slight amounts of silicon, which are the residue of ferrosilicon, i.e., the compound used during the deoxidation process, showed an effect on improving hardenability. Trace amounts of titanium and aluminium could also be distinguished in all grades. Boron, having a strong affinity for oxygen and hydrogen, reacts with these elements to form boron nitrides or oxides. Titanium and aluminium additives bind the above gases into non-metallic phases, so that an adequate amount of boron remains dissolved in the matrix, guaranteeing the material's hardenability. In addition, these compounds, forming barriers to dislocation movement, slow down austenite grain growth. Vanadium micro additive can also have a similar effect. The amount of harmful admixtures (phosphorus and sulphur) is negligible, so that high strength and ductility indices are retained.

Table 1. Chemical composition of the analyzed high-manganese steels and Hardox steels with results of hardness measurements.

	Sample 1 GX120MnCr17-2	ISO 13521:1999	Sample 2 L120G13T	PN-88/H-83160	Hardox 450	Hardox 500	Hardox 600	Hardox Extreme
C	1.23	1.20	1.10	1.00–1.40	0.17	0.29	0.44	0.45
Mn	18.00	17.50	12.50	12.00–14.00	1.00	0.74	0.53	1.00
Si	0.35	0.60	0.50	0.30–1.00	0.32	0.28	0.17	0.14
P	0.015	-	0.009	<0.100	0.010	0.007	0.006	0.006
S	0.009	-	0.008	<0.030	0.001	0.001	0.002	0.002
Cr	1.80	2.00	1.30	<1.00	0.45	0.61	0.31	0.07
Ni	0.35	-	0.50	<1.00	0.05	0.06	2.03	0.70
Mo	-	-	-	-	0.08	0.02	0.14	0.07
B	-	-	-	-	0.001	0.001	0.002	0.001
Al	-	-	-	-	0.032	0.054	0.039	0.040
Ti	-	-	-	-	0.016	0.003	0.006	0.003
V	-	-	-	-	0.005	0.012	0.006	0.008
hardness [HBW]	299	270–310	256	170–217	434	487	596	618

For microscopic studies, a Nikon Eclipse MA200 light microscope (Nikon Corporation, Tokyo, Japan) was used. Samples were examined after etching with a 3% HNO_3 solution (Mi1Fe). Nikon DS-Fi2 digital cameras, coupled to the microscopes, and Nikon's Photodocumentation NIS-Elements software (Nikon Corporation, Tokyo, Japan) were used to record and analyze images. Images of surfaces subjected to wear testing were taken with a Phenom XL electron microscope (Eindhoven, The Netherlands), using BSE imaging and a 15 keV accelerating voltage.

Examinations of abrasive wear resistance were performed using a T-07 tribotester (Radom, Poland), with loose abrasive material acc. to GOST 23.208-79 [38], under constant load F = 44 N (ΔF = 0.25 N). The T-07 tester was designed in the Institute for Sustainable

Technologies—National Research Institute in Radom. The difference between the tester T-07 and the tribotester described in the international standard ASTM G65 [39] consists in the way that locating the examined material is performed. In T-07, the specimen is placed horizontally, and in the tribotester described in ASTM, it is placed vertically. During examination, specimens sized 30 × 30 × 3 mm, made up of the research and the reference materials, were subjected to wear with abrasive particles introduced to the friction contact zone in identical working conditions, i.e., speed and load. As abrasive material, aloxite no. 90 acc. to ISO 8486-2:2007 [40] was used, and the reference specimen was made of steel C45 in an as-normalized condition. The duration of the test was selected in correspondence with the material hardness and was equal to 30 min (1800 revolutions of the roll). The coefficient of relative abrasion resistance k_b, calculated according to Formula (1), was used as a measure of abrasion resistance. The view and layout of the tester is shown in Figure 3.

$$k_b = \frac{Z_{ww}\rho_b N_b}{Z_{wb}\rho_w N_w} \quad (1)$$

where:

k_b—coefficient of relative abrasion wear resistance [dimensionless],
Z_{ww}—mass consumption of standard sample [g],
Z_{wb}—mass consumption of the tested sample [g],
N_w—the number of rotations of the rubber-rimmed steel wheel during the test of the standard sample,
N_b—the number of rotations of the rubber-rimmed steel wheel during the test of the tested sample,
ρ_w, ρ_b—material density of the standard sample and tested sample [g/cm^3].

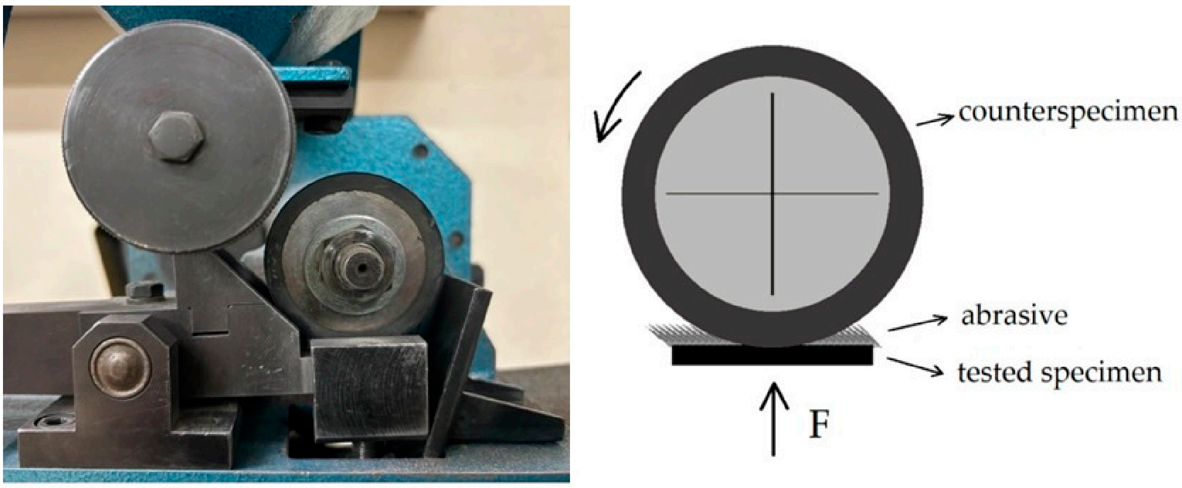

Figure 3. View and layout of the T-07 tribotester [41].

3. Results

3.1. Microstructural Analysis

Figure 4 shows the microstructures of the analyzed wear-resistant materials. Based on these images, it can be seen that samples taken from the mining equipment components show a coarse-grained austenitic microstructure, to which massive cast components were subjected due to slow cooling. In addition, precipitations of intermetallic phases were observed within the grains and at their boundaries. In an alloy containing elevated amounts of manganese and chromium (sample 1), unevenly distributed precipitations of ledeburitic carbides were also characteristic. It should be pointed out that the observed microstructural features are unfavourable from the point of view of impact strength and can cause its decrease even up to 25 J/cm^2 [42].

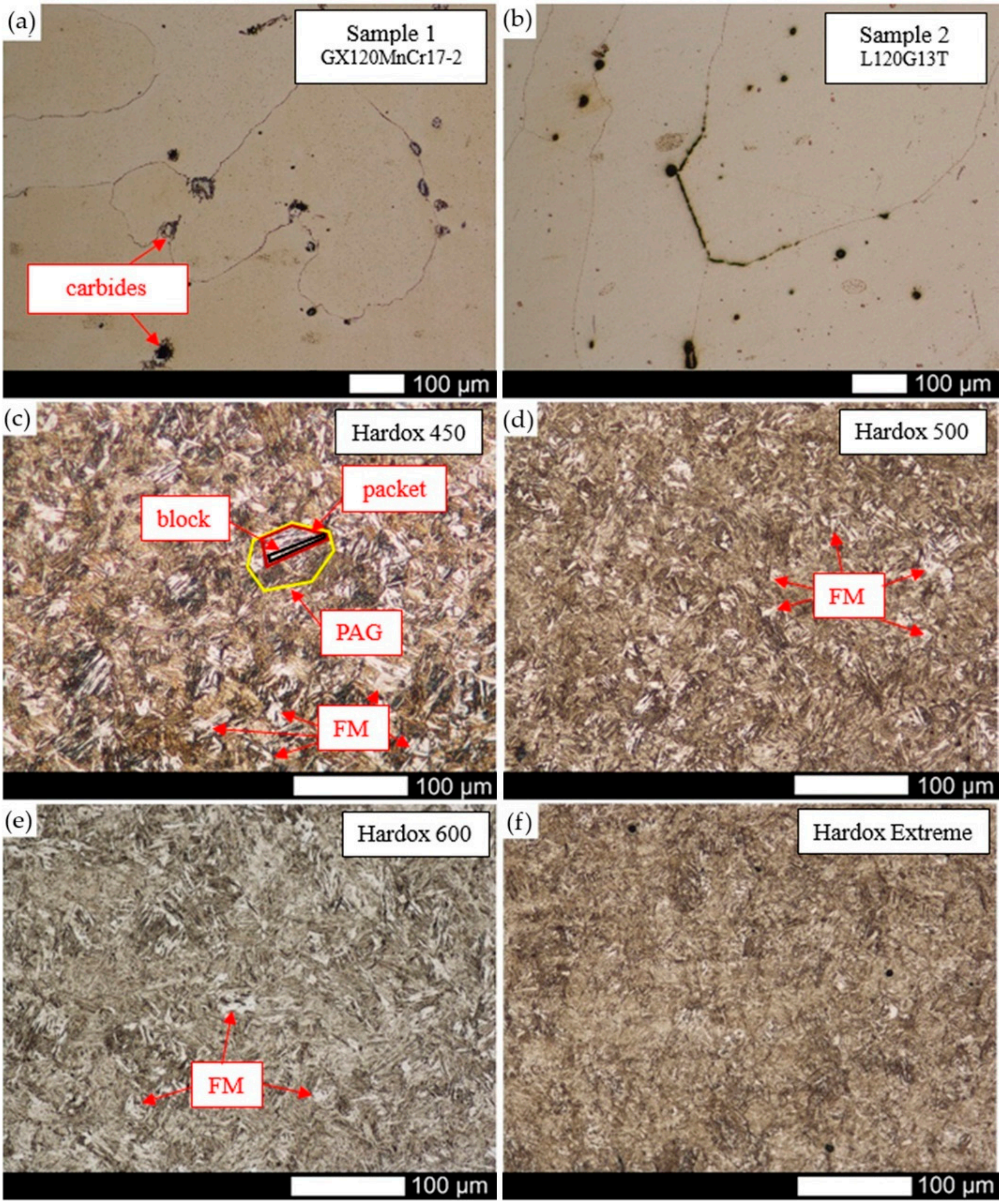

Figure 4. Microstructure of the analyzed wear-resistant materials. In the case of high-manganese cast steels (**a**,**b**), a microstructure of coarse-grained austenite with precipitations of intermetallic phases within and at grain boundaries is observed. The discontinuity of the structure—interdendritic gaps—is also characteristic. In the case of Hardox (**c**–**f**) steels, a microstructure consisting of fine lath tempering martensite with areas of hardening (fresh) martensite is observed. PAG—prior austenite grain boundary, FM—fresh martensite. Light microscopy, etched with Mi1Fe.

The microstructure of all analyzed Hardox steels is composed of homogeneous, fine lath tempering martensite. The observed structure is also characterized by a hierarchical partition, based on the division of prior austenite grains successively into packets, blocks and laths. The block-forming laths of martensite are characterized by the same crystallographic orientation and thus represent the same variant of the formed martensite microstructure. Packets, on the other hand, form clusters of blocks with the same habitus plane, corresponding to the {111} plane of primary austenite. For steels with lower carbon content, areas composed of hardening martensite are also characteristic. This is determined by the steel's lower propensity for the spontaneous tempering processes.

3.2. Abrasive Wear Resistance Tests

Abrasive wear tests showed that high-manganese steels (both GX120MnCr17-2 and L120G13T), despite their lower hardness, exhibit wear resistance comparable to Hardox 600 steel (Figure 5). The value of the coefficient k_b is equal to 1.33 (±0.03) and 1.32 (±0.01), respectively, for Hadfield steel (sample 2, designation L120G13T) and cast steel with higher chromium content (sample 1, designation GX120MnCr17-2). However, for Hardox 600 steel, the value of the coefficient k_b is 1.29 (±0.02). A slightly higher value was obtained for Hardox Extreme steel (k_b = 1.39 ± 0.02). Moreover, among Hardox steels, the relationship of hardness and wear resistance shows a linear correlation with the value of the coefficient k_b equal to 0.98 ± 0.03 and 1.14 ± 0.03, respectively, for Hardox 450 and Hardox 500 steels.

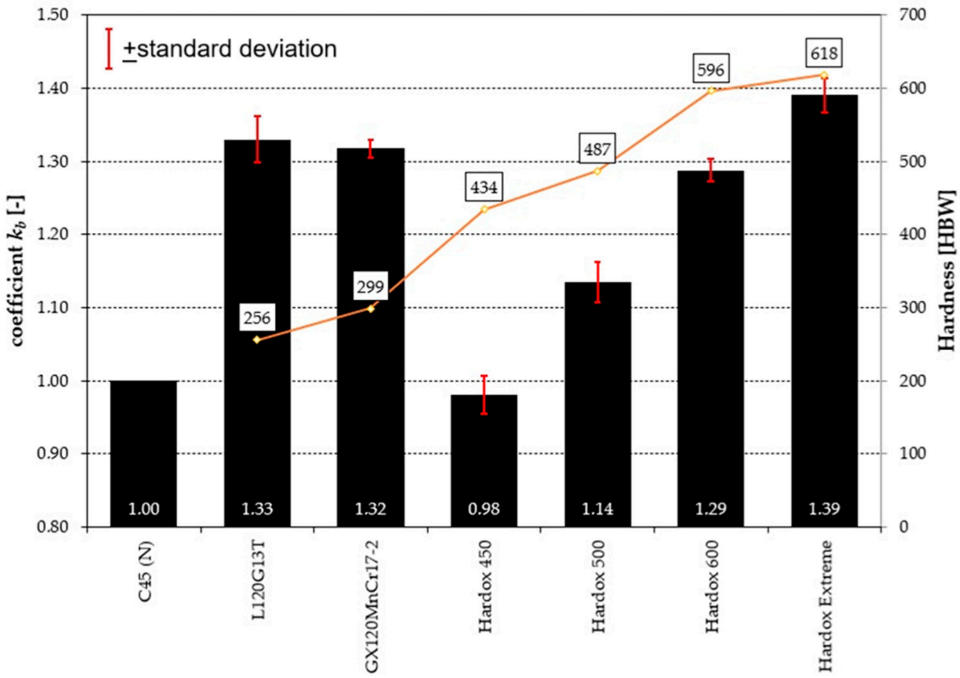

Figure 5. The value of the coefficient k_b and the results of hardness measurements of the analyzed metallic materials. C45 (N)—C45 steel in as-normalized condition with a hardness of 220 HBW.

Analysis of the surfaces of the tested materials indicated the presence of different wear mechanisms (Figure 6). In the case of high-manganese steels, the main observed wear mechanism was microploughing. There were also visible traces of impacted abrasive particles that result in occurrence of tear-outs of material in a direction disoriented from the movement of abrasive (marked as cavities). Moreover, on their edges, ridges (gouges) of plastically deformed material were present. In the case of martensitic steels, the severity of the intense changes on the surface decreased as the hardness of the material increased. The main wear mechanism of Hardox 450 and 500 steels was microploughing, plastic deformation and the breaking off of larger fragments of material, resulting in the occurrence of cavities. The formed plastic deformations were extensive and disoriented with respect to the direction of abrasive movement. The presence of pits and chips on the edges of scratches, caused by the formation of microcracks and their propagation, was also visible. Similar traces could be observed in Hardox 600 and Hardox Extreme steels, but the width of the plastic deformations, grooves, breakouts and scratches were smaller. Moreover, the proportion of wear by microploughing decreased, and the material was mainly worn by microcutting.

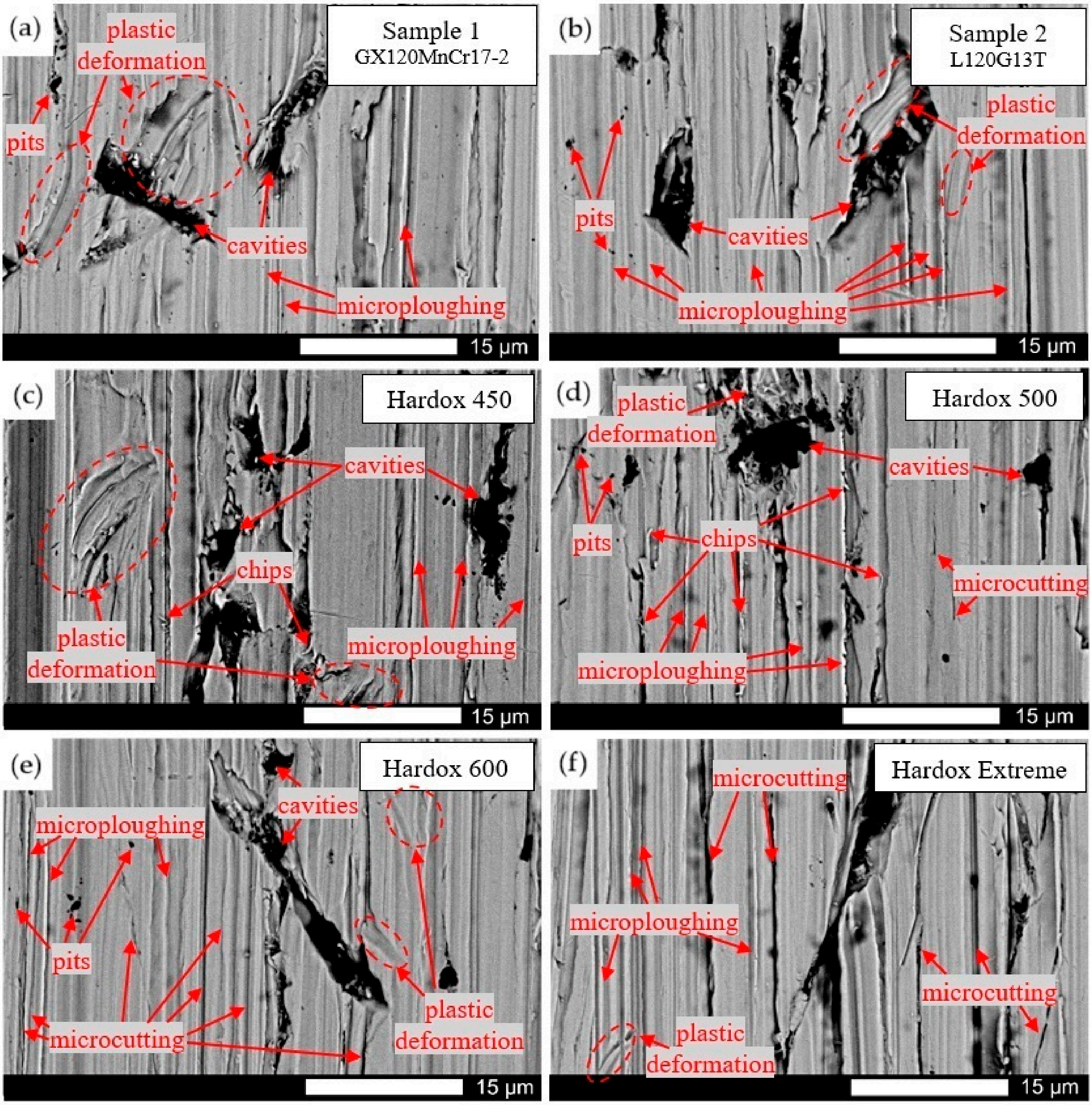

Figure 6. Surfaces subjected to wear testing: (**a**) sample 1 (GX120MnCr17-2); (**b**) sample 2 (L120G13T); (**c**) Hardox 450; (**d**) Hardox 500; (**e**) Hardox 600; (**f**) Hardox Extreme. Electron microscopy, unetched.

It should be noted that, according to the analysis of microstructural changes in the subsurface layers of the samples subjected to wear tests (Figure 7), high-manganese steels had the greatest change in profile height, which could be up to 9 μm. Their surfaces were smooth and only locally sharply defined pits could be observed. In the case of Hardox 450 and Hardox 500 steels, the deformation of the microstructure under the influence of the movement of abrasive grains under pressure was characteristic. Smoothly finished material breakouts and grooves could also be observed. Deformation of martensitic microstructure is also relevant to Hardox 600 steel. However, the presence of sharply ended breakouts indicated an increased contribution of microcutting to the wear mechanisms taking place. Moreover, the resulting pits were narrower and shallower compared to Hardox 450 and 500 steels. In the case of Hardox Extreme steels, the texture was less favoured and oriented (directed). The resulting pits were shallower compared to the other steels. The smooth surface was indicative of the uniform abrasion of the surface as a result of microcutting.

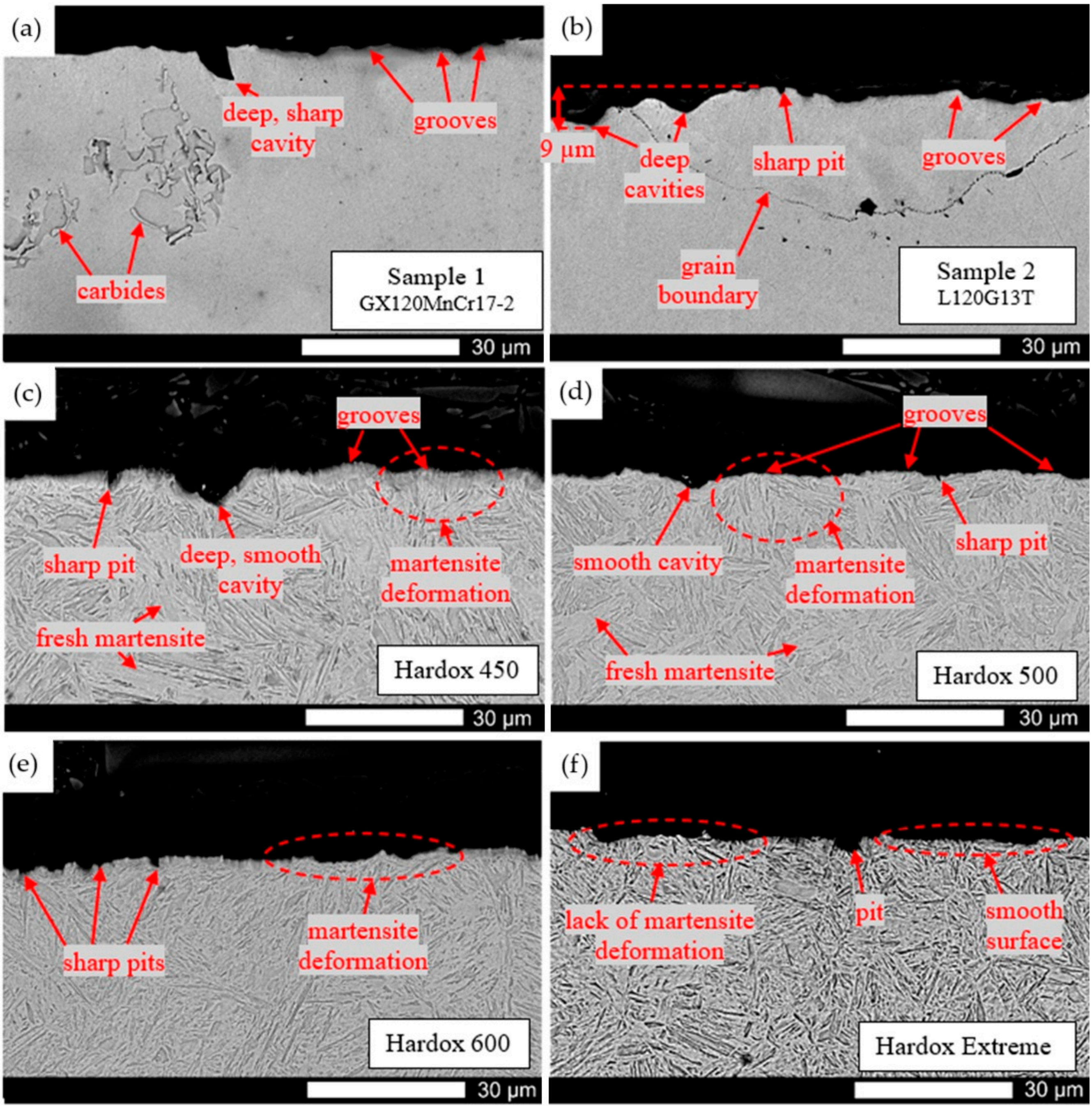

Figure 7. Microstructure of the subsurface area of specimens subjected to wear tests in the direction transverse to the abrasive movement: (**a**) sample 1 (GX120MnCr17-2); (**b**) sample 2 (L120G13T); (**c**) Hardox 450; (**d**) Hardox 500; (**e**) Hardox 600; (**f**) Hardox Extreme. Electron microscopy, etched with Mi1Fe.

4. Discussion

This paper presents the results of abrasive wear testing of Hardox steel and Hadfield cast steel, which was taken from equipment components used in the mining industry. According to the presented results, the abrasive wear of high-manganese steel is comparable with the resistance of Hardox 600 steel. In martensitic steels, the relationship of hardness and abrasive wear resistance shows a linear correlation. The comparable resistance of steels with a hardness not exceeding 450 HBW and C45 steel in the as-normalized condition (hardness of 220 HBW) is determined by the wear mechanism. C45 steel is composed of 50% ferrite, which undergoes plastic deformation, and the increase in resistance is only pronounced for steel with a hardness of 500 HBW, as it was already noted in the [43]. Also, according to the results presented in [44,45], steel with ferritic-pearlitic-bainitic microstructure may show an advantage over martensitic steel. In this case, the main wear mechanism is microploughing, and mass loss occurs only as a result of repeated plastic deformation of the material and thus its mechanical strengthening. Microploughing alone—unlike microcutting—does not result in mass loss, and caution should be exercised within ferrite-containing steels when evaluating abrasive wear resistance as a function of mass loss. However, it is not always the case, and Hardox 450 steel is considered more advantageous in terms of abrasive wear resistance in comparison to S355J2G3 steel [34]. The obtained correlation between hardness and abrasive wear resistance is consistent with the results presented in [46]. In the aforementioned work, Bialobrzeska studied eight steels with carbon contents in the range of 0.31–0.41 wt%, which were characterized by different content of manganese, chromium, vanadium, as well as boron. All the materials were hardened to a martensite microstructure, and in this state their wear intensity was related to carbon content and hardness, and, in the course of later studies, to yield strength [47]. In the paper [48], five commercially available martensitic steels with hardnesses of 400, 500 (three types) and 600 HBW were tested. Each of the used test methods (crushing pin-on-disc, high-speed slurry-pot and impeller-tumbler device) conditioned the generation of high stresses that led to the crushing of the abrasive, plastic deformation of the tested surface and the formation of adiabatic shear bands inside the material. Nevertheless, in each case, the steel with a hardness of 400 HBW showed the least favourable wear rates, while the steel with a hardness of 600 HBW exhibited the lowest mass consumption. In the work [33], the material with the highest hardness of 49.9 HRC (the steel used for ploughshares by Lemken) also showed the most advantageous wear resistance, both in laboratory and field tests. However, in the work presented here, within the martensitic microstructures, the relationship between hardness and abrasive wear resistance was not observed. Hardox 500 steel (hardness of 47.1 HRC) showed higher wear rates compared to B27 steel (hardened state with a hardness of 45.7 HRC and low-tempered state with a hardness of 44.2 HRC), which was associated with a change in the nature of wear. The problem of uneven behaviour of different steels with a hardness of 400 HBW, which is caused by the strengthening of subsurface layers due to plastic deformation, is also pointed out by the authors of the paper [49–51]. Nevertheless, in the above cases, the variation in hardness between the analyzed grades does not exceed 50 Brinell units, and clarification of these relationships requires further research related to the correlation of microstructural and mechanical properties with chemical composition.

It should be noted that the relationship of hardness and wear resistance within martensitic steels seems reasonable only for loose (dry) abrasive (Figure 8). According to the results of the study presented in [52], Hardox 600 steel shows more favourable wear rates compared to Hardox Extreme steel in the presence of soil abrasive mass. The authors related the obtained results to the nature of the abrasive (its bonding and grain size) and the plastic deformation of the material with martensitic microstructure. Comparing the above results with those presented in the [53–56], it should be pointed out that the correlation between hardness and wear resistance is not valid in the presence of an abrasive medium that poses a higher friction resistance, taking into account the medium abrasive soil mass (Figure 9). In this case, higher strength steels (Hardox Extreme, XAR 600, 38GSA) have lower wear resistance compared to Brinar 400, Brinar 500, B27 or Creusabro 4800 steels. The medium soil, through its increased content of clay causing bonding of hard abrasive particles, has significantly reduced degrees of freedom of sand grains and acts with greater force on the tested surface [57,58]. Therefore, it can be concluded that wear resistance is strongly dependent on the type of abrasive, and in the case of a dry and loose medium, it is the hardness that shows a dominant influence on the obtained values.

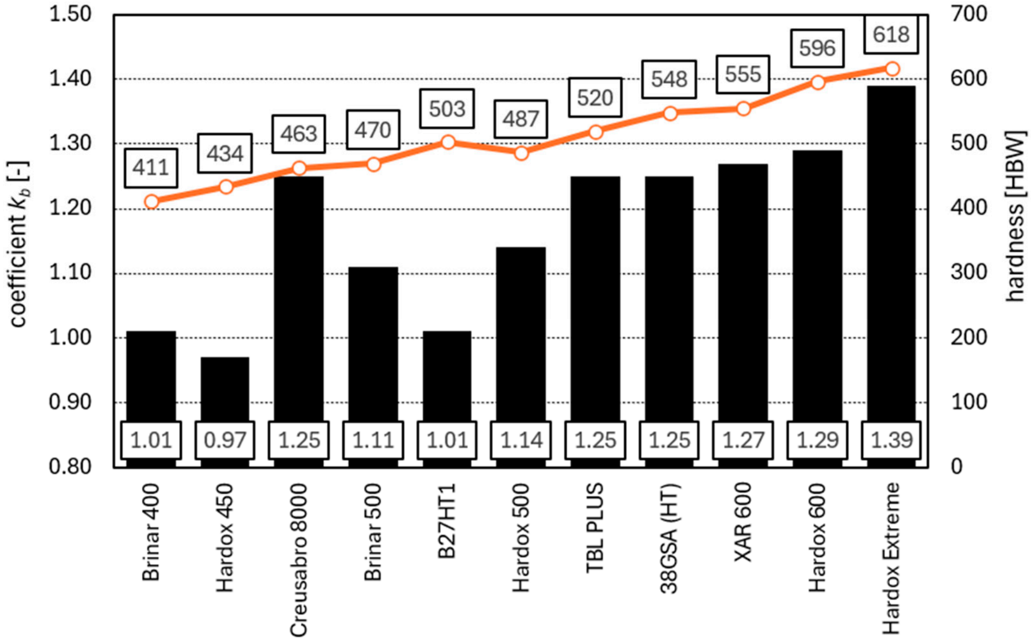

Figure 8. Coefficient of relative abrasion wear resistance k_b and results of hardness measurements of selected low-alloyed martensitic steels. HT-heat-treated. Based on the results presented in this paper and [33,41,43].

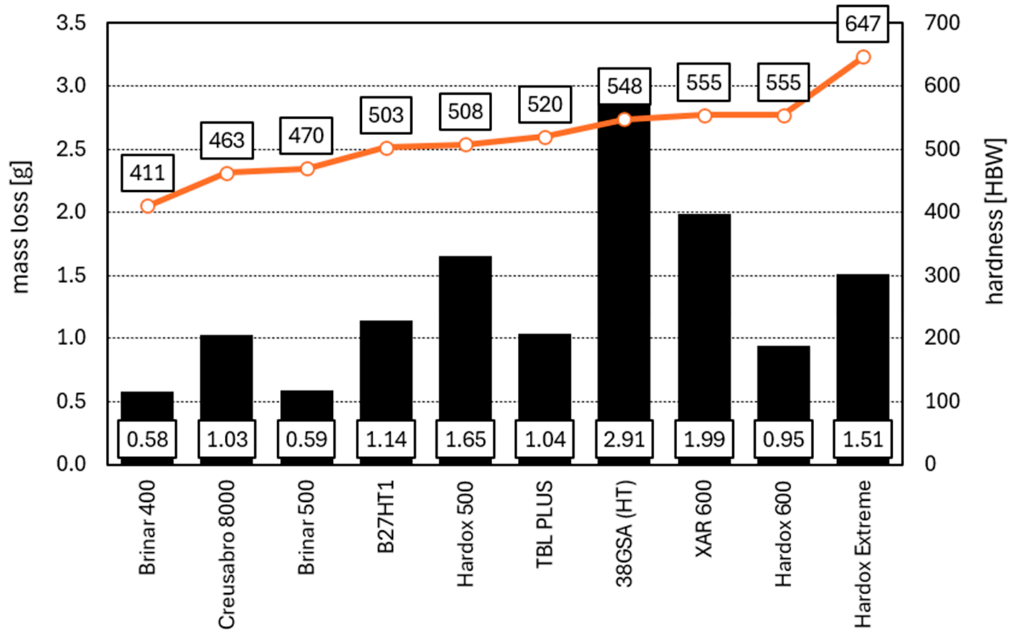

Figure 9. Resistance to abrasive wear in medium abrasive soil mass over the friction path of 20 km and results of hardness measurements of selected low-alloyed martensitic steels. HT-heat-treated. Based on [52–56].

In the case of high-manganese steel, the values of the coefficient k_b are similar to the results obtained for Hardox 600. As in the case of Creusabro steel, which is characterized by the presence of residual austenite [41], their high resistance is determined by the significant plastic deformation of the material and the predominant wear mechanism by microploughing. What is more, no significant differences in abrasive wear resistance were observed between the cast steel of basic chemical composition and the one with added chromium. It should be noted that, according to [59,60], the above relationship can only be verified by increasing the clamping force of the countersample and extending the test time. In the analyzed case, when the applied load was 500 N, no clear differences in weight loss were observed between Mn12 and Mn12CrN steel. Only as the test time was extended beyond 60 min and the pressure was increased to 1000 N, did the chromium-nitrogen steel begin to show more favourable wear rates due to a higher degree of strengthening of the subsurface layers. As it was shown, a rapid hardening effect that affects higher wear resistance could be obtained in the Mn12CrN steel only under higher applied wear load.

Hadfield steel is characterized by difficult weldability, and due to its tendency to coarse-graining and the lack of α -> γ transformation, it becomes practically impossible to implement heat treatment procedures aimed at fragmenting the structure. In this case, according to the results presented in the above paper, it is the high-strength boron martensitic steels that can provide an alternative, with similar wear resistance indices of Hadfield steel and Hardox 600 steel. The results obtained in this manuscript are consistent with the results of the work presented in [61], where the abrasive wear resistance of Hardox 450 steel was lower compared to MMA (medium-manganese austenitic) steel, during both sliding tribocorrosion and impact tribocorrosion tests. Hardox 450 steel also showed higher weight loss relative to Hadfield steel during tests reported in [62], where the abrasive was light stony soil, but in this case, it was the resistance of B27 steel (which is supplied in as-normalized state and intended for subsequent implementation of heat treatment procedures to achieve mechanical properties similar to Hardox 500), that proved to be the highest. However, the authors did not carry out material testing and the state of the heat treatment was not reported. Hadfield steel, also in dry sliding and salt-water sliding conditions [63] or during dry friction [64], shows an advantage over martensitic steel with a hardness of 500 HBW. Nevertheless, as a result of the change in the properties of the surface layers of Hadfield steel, contributing to an increase in the proportion of wear by microcutting with an increase in the magnitude of the applied load from 10 N to 45 N during tests conducted using "steel disc-abrasive-abraded material" friction pairs, Hadfield steel alloyed with various additives (Ni, Cr, Mo, Si, Cu, B and/or WC) showed similar wear rates compared to Hardox 400 [65]. The above statement is also valid under the conditions of tribological tests such as abrasive–erosive wear and surface fatigue wear [66].

On the basis of the conducted tests and comparison of the obtained results with the available literature sources, it should be concluded that Hadfield cast steel under abrasive wear conditions shows advantages over steel of 500 HBW hardness and can be used interchangeably with steel of 600 HBW hardness. However, it is steel of 650 HBW hardness that shows the most favourable indices. In this case, recommended applications include components subjected to significant surface pressure, such as screed and liner plates or belts used for handling crushed (ground) materials. Hadfield steel is more practical for use in cast components, considering primarily crusher jaws, for which contouring the surface to the required shapes is difficult due to material strengthening during machining. Under dynamic loading conditions, Hardox 500 (KCV_{+20} = 60 J/cm^2) or Hardox 600 steel (KCV_{+20} = 40 J/cm^2) may show more favourable properties due to the possible decrease in impact strength of Hadfield steel up to 25 J/cm^2, conditioned by the coarse-grained structure and carbide separations at grain boundaries [42]. Such components include bucket wheel chutes, excavator bucket components or transfers, but in this case, the next research step should be bench tests conducted to fully evaluate the serviceability of the analyzed materials. In addition, due to the nature of the conducted test, Hardox 500 and Hardox 600 steels are recommended for components designed for light soil abrasion (classified in a number of standards), including ploughshares and cultivator ridges. Light soils involve soils with a higher content of dry and loose sand, while heavier soils have higher amounts of flowable fractions (dust and silt, causing grains bonding). Due to the nature of the work, Hardox steel is preferable to Hadfield steel in this case-, what is determined by its -uniform mechanical properties across the material.

5. Conclusions

Based on the presented results of the study, the following conclusions can be drawn:

- The microstructure of the analyzed high-manganese steels, used for parts of the components in the mining industry, is composed of coarse-grained austenite with precipitations of intermetallic phases within the grains and at their boundaries. Locally, uncrystallized interdendritic spaces can be seen. The hardness is 299 HBW (sample 1, designation GX120MnCr17-2) and 256 HBW (sample 2, designation L120G13T).
- The microstructure of Hardox steels is composed of fine lath tempering martensite; however, in the case of steels with lower carbon content, i.e., Hardox 450 and Hardox 500, some areas of hardening martensite are observed. Hardness is in the range of 434–618 HBW.
- Abrasive wear resistance tests performed in the presence of a loose abrasive (electrocorundum) show a linear relationship with respect to hardness within the martensitic microstructures. On the other hand, both tested high-manganese steels show similar wear rates to Hardox 600, that is to a steel with a hardness of 600 HBW.
- The main wear mechanism of high-manganese steels is microploughing, plastic deformation and breakouts of larger fragments of material. In the case of Hardox 450 and Hardox 500 steels, the predominant wear mechanisms are microploughing and breaking out of material fragments. As the hardness of the steel increases, the proportion of wear by microcutting and scratching predominates.
- The above observations are confirmed by images of cross sections of surfaces subjected to wear tests. The greatest change in profile height, width of grooves and their depth is characterized by high-manganese steel. For Hardox 450 and Hardox 500 steels, the deformation of the microstructure under the influence of the movement of abrasive grains under pressure is characteristic. For Hardox 600 and Hardox Extreme steels, sharp edges are observed, the resulting pits are narrower and shallower, and the texture is less favoured and oriented (directed).

Author Contributions: Conceptualization, M.Z. and Ł.K.; methodology, M.Z., K.L. and Ł.K.; validation, M.Z. and Ł.K.; formal analysis, M.Z. and Ł.K.; investigation, M.Z. and K.L.; resources, Ł.K., M.Z. and K.L.; data curation, M.Z.; writing—original draft preparation, M.Z.; writing—review and editing, Ł.K. and K.J.; visualization, M.Z.; supervision, Ł.K. and K.J.; funding acquisition, K.J. All authors have read and agreed to the published version of the manuscript.

Funding: This research received no external funding.

Institutional Review Board Statement: Not applicable.

Informed Consent Statement: Not applicable.

Data Availability Statement: The original contributions presented in the study are included in the article, further inquiries can be directed to the corresponding authors.

Conflicts of Interest: The authors declare no conflicts of interest.

References

1. Rojacz, H.; Katsich, C.; Kirchgaßner, M.; Kirchmayer, R.; Badisch, E. Impact-Abrasive Wear of Martensitic Steels and Complex Iron-Based Hardfacing Alloys. *Wear* **2022**, *492–493*, 204183. [CrossRef]
2. Ratia, V.; Rojacz, H.; Terva, J.; Valtonen, K.; Badisch, E.; Kuokkala, V.-T. Effect of Multiple Impacts on the Deformation of Wear-Resistant Steels. *Tribol. Lett.* **2015**, *57*, 15. [CrossRef]
3. Valtonen, K.; Keltamäki, K.; Kuokkala, V.-T. High-Stress Abrasion of Wear Resistant Steels in the Cutting Edges of Loader Buckets. *Tribol. Int.* **2018**, *119*, 707–720. [CrossRef]

4. Haiko, O.; Javaheri, V.; Valtonen, K.; Kaijalainen, A.; Hannula, J.; Kömi, J. Effect of Prior Austenite Grain Size on the Abrasive Wear Resistance of Ultra-High Strength Martensitic Steels. *Wear* **2020**, *454–455*, 203336. [CrossRef]
5. Haimann, R. *Metaloznawstwo*; Wydawnictwo Politechniki Wrocławskiej: Wrocław, Poland, 1980.
6. Yan, W.; Fang, L.; Sun, K.; Xu, Y. Effect of Surface Work Hardening on Wear Behavior of Hadfield Steel. *Mater. Sci. Eng. A* **2007**, *460–461*, 542–549. [CrossRef]
7. Najafabadi, V.N.; Amini, K.; Alamdarlo, M.B. Investigating the Effect of Titanium Addition on the Wear Resistance of Hadfield Steel. *Metall. Res. Technol.* **2014**, *111*, 375–382. [CrossRef]
8. Ayadi, S.; Hadji, A. Effect of Heat Treatments on the Microstructure and Wear Resistance of a Modified Hadfield Steel. *Metallofiz. Noveishie Tekhnol.* **2019**, *41*, 607–620. [CrossRef]
9. Abbasi, M.; Kheirandish, S.; Kharrazi, Y.; Hejazi, J. On the Comparison of the Abrasive Wear Behavior of Aluminum Alloyed and Standard Hadfield Steels. *Wear* **2010**, *268*, 202–207. [CrossRef]
10. Abbasi, M.; Kheirandish, S.; Kharrazi, Y.; Hejazi, J. The Fracture and Plastic Deformation of Aluminum Alloyed Hadfield Steels. *Mater. Sci. Eng. A* **2009**, *513–514*, 72–76. [CrossRef]
11. Tęcza, G. Changes in Microstructure and Abrasion Resistance during Miller Test of Hadfield High-Manganese Cast Steel after the Formation of Vanadium Carbides in Alloy Matrix. *Materials* **2022**, *15*, 1021. [CrossRef] [PubMed]
12. Tęcza, G. Changes in Abrasive Wear Resistance during Miller Test of High-Manganese Cast Steel with Niobium Carbides Formed in the Alloy Matrix. *Appl. Sci.* **2021**, *11*, 4794. [CrossRef]
13. Dziubek, M.; Rutkowska-Gorczyca, M.; Dudziński, W.; Grygier, D. Investigation into Changes of Microstructure and Abrasive Wear Resistance Occurring in High Manganese Steel X120Mn12 during Isothermal Annealing and Re-Austenitisation Process. *Materials* **2022**, *15*, 2622. [CrossRef] [PubMed]
14. SSAB. SSAB High-Strength Steel—Sheet, Plate, Coil, Tube, Profile. 2021. Available online: https://www.ssab.com/en/brands-and-products/hardox (accessed on 25 August 2024).
15. Białobrzeska, B.; Jasiński, R.; Konat, Ł.; Szczepański, Ł. Analysis of the Properties of Hardox Extreme Steel and Possibilities of Its Applications in Machinery. *Metals* **2021**, *11*, 162. [CrossRef]
16. Prochenka, P.; Janiszewski, J.; Kucewicz, M. Crash Response of Laser-Welded Energy Absorbers Made of Docol 1000DP and Docol 1200M Steels. *Materials* **2021**, *14*, 2808. [CrossRef] [PubMed]
17. Barnes, N.; Joseph, T.; Mendez, P.F. Issues Associated with Welding and Surfacing of Large Mobile Mining Equipment for Use in Oil Sands Applications. *Sci. Technol. Weld. Join.* **2015**, *20*, 483–493. [CrossRef]
18. Kowalczyk, M.; Czmochowski, J.; Rusiński, E. Construction of Diagnostic Models of the States of Developing Fault for Working Parts of the Multi-Bucket Excavator. *Ekspolat. Niezawodn.—Maint. Reliab.* **2009**, *11*, 17–24.
19. Hryciów, Z.; Małachowski, J.; Rybak, P.; Wiśniewski, A. Research of Vibrations of an Armoured Personnel Carrier Hull with FE Implementation. *Materials* **2021**, *14*, 6807. [CrossRef] [PubMed]
20. Zochowski, P.; Bajkowski, M.; Grygoruk, R.; Magier, M.; Burian, W.; Pyka, D.; Bocian, M.; Jamroziak, K. Comparison of Numerical Simulation Techniques of Ballistic Ceramics under Projectile Impact Conditions. *Materials* **2021**, *15*, 18. [CrossRef] [PubMed]
21. Popławski, A.; Kędzierski, P.; Morka, A. Identification of Armox 500T Steel Failure Properties in the Modeling of Perforation Problems. *Mater. Des.* **2020**, *190*, 108536. [CrossRef]
22. Białobrzeska, B.; Jasiński, R.; Dziurka, R.; Bała, P. Effect of Chromium and Titanium on the Microstructure and Mechanical Properties of Cast Steel. *J. Min. Metall. Sect. B Metall.* **2024**, *60*, 235–237. [CrossRef]
23. Silva, A.P.; Węgrzyn, T.; Szymczak, T.; Szczucka-Lasota, B.; Łazarz, B. Hardox 450 Weld in Microstructural and Mechanical Approaches after Welding at Micro-Jet Cooling. *Materials* **2022**, *15*, 7118. [CrossRef] [PubMed]
24. Uzunali, U.Y.; Cuvalcı, H.; Atmaca, B.; Demir, S.; Özkaya, S. Mechanical Properties of Quenched and Tempered Steel Welds. *Mater. Test.* **2022**, *64*, 1662–1674. [CrossRef]
25. Krawczyk, R.; Słania, J.; Golański, G.; Zieliński, A. Evaluation of the Properties and Microstructure of Thick-Walled Welded Joint of Wear Resistant Materials. *Materials* **2022**, *15*, 7009. [CrossRef] [PubMed]
26. Teker, T.; Gencdogan, D. Heat Affected Zone and Weld Metal Analysis of HARDOX 450 and Ferritic Stainless Steel Double Sided TIG-Joints. *Mater. Test.* **2021**, *63*, 923–928. [CrossRef]
27. Baskutis, S.; Baskutiene, J.; Dragašius, E.; Kavaliauskiene, L.; Keršiene, N.; Kusyi, Y.; Stupnytskyy, V. Influence of Additives on the Mechanical Characteristics of Hardox 450 Steel Welds. *Materials* **2023**, *16*, 5593. [CrossRef] [PubMed]
28. Zemlik, M.; Konat, Ł.; Białobrzeska, B. Analysis of the Possibilities to Increase Abrasion Resistance of Welded Joints of Hardox Extreme Steel. *Tribol. Int.* **2025**, *201*, 110271. [CrossRef]
29. Mukhamedov, A.A. Strength and Wear Resistance in Relation to the Austenite Grain Size and Fine Structure of the Steel. *Met. Sci. Heat Treat.* **1968**, *10*, 526–528. [CrossRef]
30. Białobrzeska, B.; Dziurka, R.; Żak, A.; Bała, P. The Influence of Austenitization Temperature on Phase Transformations of Supercooled Austenite in Low-Alloy Steels with High Resistance to Abrasion Wear. *Arch. Civ. Mech. Eng.* **2018**, *18*, 413–429. [CrossRef]
31. Tarasiuk, W.; Napiórkowski, J.; Ligier, K.; Krupicz, B. Comparison of the Wear Resistance of Hardox 500 Steel and 20MnCr5. *Tribologia* **2017**, *273*, 165–170. [CrossRef]
32. Szala, M.; Szafran, M.; Macek, W.; Marchenko, S.; Hejwowski, T. Abrasion Resistance of S235, S355, C45, AISI 304 and Hardox 500 Steels with Usage of Garnet, Corundum and Carborundum Abrasives. *Adv. Sci. Technol. Res. J.* **2019**, *13*, 151–161. [CrossRef]

33. Białobrzeska, B.; Kostencki, P. Abrasive Wear Characteristics of Selected Low-Alloy Boron Steels as Measured in Both Field Experiments and Laboratory Tests. *Wear* **2015**, *328–329*, 149–159. [CrossRef]
34. Vargova, M.; Tavodova, M.; Monkova, K.; Dzupon, M. Research of Resistance of Selected Materials to Abrasive Wear to Increase the Ploughshare Lifetime. *Metals* **2022**, *12*, 940. [CrossRef]
35. *ISO 6506-1:2014*; Metallic Materials—Brinell Hardness Test—Part 1: Test Method. International Organization for Standardization: Geneva, Switzerland, 2014.
36. *PN-88/H-83160*; Staliwo odporne na ścieranie—Gatunki. Polski Komitet Normalizacji: Miar i Jakości, Polska, 1988.
37. *ISO 13521:1999*; Austenitic Manganese Steel Castings. International Organization for Standardization: Geneva, Switzerland, 1999.
38. *GOST 23.208-79*; Ensuring of wear resistance of products. Wear resistance testing of materials by friction against loosely fixed abrasive particles. Rosstandart: Moscow, Russian, 1979.
39. *ASTM G65-16(2021)*; Standard Test Method for Measuring Abrasion Using the Dry Sand/Rubber Wheel Apparatus. ASTM International: West Conshohocken, PA, USA, 2021.
40. *ISO 8486-2:2007*; Bonded abrasives—Determination and Designation of Grain Size Distribution—Part 2: Microgrits F230 to F2000. International Organization for Standardization: Geneva, Switzerland, 2007.
41. Zemlik, M.; Konat, Ł.; Napiórkowski, J. Comparative Analysis of the Influence of Chemical Composition and Microstructure on the Abrasive Wear of High-Strength Steels. *Materials* **2022**, *15*, 5083. [CrossRef]
42. Tęcza, G.; Zapała, R. Changes in Impact Strength and Abrasive Wear Resistance of Cast High Manganese Steel Due to the Formation of Primary Titanium Carbides. *Arch. Foundry Eng.* **2018**, *18*, 119–122.
43. Białobrzeska, B.; Konat, Ł. Comparative Analysis of Abrasive-Wear Resistance of Brinar and Hardox Steels. *Tribologia* **2017**, *272*, 7–16. [CrossRef]
44. Sundström, A.; Rendón, J.; Olsson, M. Wear Behaviour of Some Low Alloyed Steels under Combined Impact/Abrasion Contact Conditions. *Wear* **2001**, *250*, 744–754. [CrossRef]
45. Rendón, J.; Olsson, M. Abrasive Wear Resistance of Some Commercial Abrasion Resistant Steels Evaluated by Laboratory Test Methods. *Wear* **2009**, *267*, 2055–2061. [CrossRef]
46. Białobrzeska, B. The Influence of Boron on the Resistance to Abrasion of Quenched Low-Alloy Steels. *Wear* **2022**, *500–501*, 204345. [CrossRef]
47. Białobrzeska, B.; Jasiński, R. Resistance to Abrasive Wear with Regards to Mechanical Properties Using Low-Alloy Cast Steels Examined with the Use of a Dry Sand/Rubber Wheel Tester. *Materials* **2023**, *16*, 3052. [CrossRef]
48. Valtonen, K.; Ojala, N.; Haiko, O.; Kuokkala, V.-T. Comparison of Various High-Stress Wear Conditions and Wear Performance of Martensitic Steels. *Wear* **2019**, *426–427*, 3–13. [CrossRef]
49. Ojala, N.; Valtonen, K.; Heino, V.; Kallio, M.; Aaltonen, J.; Siitonen, P.; Kuokkala, V.-T. Effects of Composition and Microstructure on the Abrasive Wear Performance of Quenched Wear Resistant Steels. *Wear* **2014**, *317*, 225–232. [CrossRef]
50. Mondal, J.; Das, K.; Das, S. An Investigation of Mechanical Property and Sliding Wear Behaviour of 400Hv Grade Martensitic Steels. *Wear* **2020**, *458–459*, 203436. [CrossRef]
51. Jafari, A.; Dehghani, K.; Bahaaddini, K.; Abbasi Hataie, R. Experimental Comparison of Abrasive and Erosive Wear Characteristics of Four Wear-Resistant Steels. *Wear* **2018**, *416–417*, 14–26. [CrossRef]
52. Ligier, K.; Zemlik, M.; Lemecha, M.; Konat, Ł.; Napiórkowski, J. Analysis of Wear Properties of Hardox Steels in Different Soil Conditions. *Materials* **2022**, *15*, 7622. [CrossRef]
53. Konat, Ł.; Napiórkowski, J.; Białobrzeska, B. Structural Properties and Abrasive-Wear Resistance of Brinar 400 and Brinar 500 Steels. *Tribologia* **2017**, *273*, 67–75. [CrossRef]
54. Konat, Ł.; Napiórkowski, J.; Kołakowski, K. Resistance to Wear as a Function of the Microstructure and Selected Mechanical Properties of Microalloyed Steel with Boron. *Tribologia* **2016**, *268*, 101–114. [CrossRef]
55. Napiórkowski, J.; Konat, Ł.; Ligier, K. The Structural Properties and Resistance to Abrasive Wear in Soil of Creusabro Steel. *Tribologia* **2016**, *269*, 105–119. [CrossRef]
56. Konat, Ł.; Napiórkowski, J. The Effect of the Method and Parameters of the Heat Treatment on Abrasive Wear Resistance of 38GSA Steel. *Tribologia* **2019**, *285*, 61–69. [CrossRef]
57. Lemecha, M.; Ligier, K.; Napiórkowski, J.; Vrublevskyi, O. Analysis of Tribological Properties of Hardfaced High-Chromium Layers Subjected to Wear in Abrasive Soil Mass. *Materials* **2024**, *17*, 3461. [CrossRef]
58. Lemecha, M.; Napiórkowski, J.; Ligier, K.; Tarasiuk, W.; Sztukowski, K. Analysis of Wear Properties of Powder Metallurgy Steel in Abrasive Soil Mass. *Materials* **2022**, *15*, 6888. [CrossRef]
59. Chen, C.; Lv, B.; Ma, H.; Sun, D.; Zhang, F. Wear Behavior and the Corresponding Work Hardening Characteristics of Hadfield Steel. *Tribol. Int.* **2018**, *121*, 389–399. [CrossRef]
60. Lindroos, M.; Apostol, M.; Heino, V.; Valtonen, K.; Laukkanen, A.; Holmberg, K.; Kuokkala, V.-T. The Deformation, Strain Hardening, and Wear Behavior of Chromium-Alloyed Hadfield Steel in Abrasive and Impact Conditions. *Tribol. Lett.* **2015**, *57*, 24. [CrossRef]
61. Tan, N.; Qiao, J.; Wang, Q. Tribocorrosion Performance of Medium-Manganese Austenitic Wear-Resistant Steel in Simulated Mine Water. *Corros. Sci.* **2023**, *219*, 111225. [CrossRef]
62. Kaminski, J.; Sypula, M.; Chlebowski, J.; Nowakowski, T. Research in Rake Tines Wear. Available online: https://www.iitf.lbtu.lv/conference/proceedings2018/Papers/N077.pdf (accessed on 25 August 2024).

63. Podgornik, B.; Vizintin, J.; Thorbjornsson, I.; Johannesson, B.; Thorgrimsson, J.T.; Martinez Celis, M.; Valle, N. Improvement of Ductile Iron Wear Resistance through Local Surface Reinforcement. *Wear* **2012**, *274–275*, 267–273. [CrossRef]
64. Bolobov, V.I.; Chupin, S.A.; Bochkov, V.S.; Akhmerov, E.V.; Plaschinskiy, V.A. The Effect of Finely Divided Martensite of Austenitic High Manganese Steel on the Wear Resistance of the Excavator Buckets Teeth. *Key Eng. Mater.* **2020**, *854*, 3–9. [CrossRef]
65. Jankauskas, V.; Katinas, E.; Varnauskas, V.; Katinas, A.; Antonov, M. Assessment of the Reliability of Hardfacings for Soil Rippers. *J. Frict. Wear* **2015**, *36*, 89–95. [CrossRef]
66. Kulu, P.; Veinthal, R.; Saarna, M.; Tarbe, R. Surface Fatigue Processes at Impact Wear of Powder Materials. *Wear* **2007**, *263*, 463–471. [CrossRef]